

# Novel Polymeric Materials with Double Porosity: Synthesis and Characterization

*Benjamin Le Droumaguet, Romain Lacombe, Hai-Bang Ly, Benjamin Carbonnier, Daniel Grande\**

**Summary:** This paper reports on two straightforward and versatile routes to functional doubly porous polymeric materials based on cross-linked poly(2-hydroxyethyl methacrylate) (PHEMA) via novel porogen templating methodologies. The quantitative removal of either  $\text{CaCO}_3$  particles or poly(methyl methacrylate) beads as macroporogens, in conjunction with either hydroxyapatite nanoparticles or a solvent as nanoporogens, led to the generation of macropores with dimensions in the 100  $\mu\text{m}$  range, while the second porosity lied within the 1  $\mu\text{m}$  order of magnitude, as evidenced by mercury intrusion porosimetry and scanning electron microscopy. The successful functionalization of such doubly porous PHEMA-based frameworks was implemented through a straightforward two-step chemical modification involving an activation stage, followed by the coupling of propargylamine as a model compound. Raman spectroscopy clearly indicated the occurrence of alkyne functionality within the biporous materials.

**Keywords:** doubly porous materials; macroporogen; nanoporogen; poly(2-hydroxyethyl methacrylate); surface functionalization

## Introduction

Porous materials – either organic or inorganic<sup>[1]</sup> – have been the subject of intense research for many years, mainly because of their wide range of applications. Polymer-based porous materials have particularly attracted much interest from the research community,<sup>[2]</sup> as they possess some undeniable advantages over their inorganic counterparts. First, they display tunable mechanical properties in a useful range. Second, they can easily be functionalized by simple organic reactions. Last but not least, they can be engineered by processes with very low production costs. Among the plethora of porous polymeric materials, those based on biocompatible polymers, such as poly(lactic acid) or poly(lactic acid-co-glycolic acid) (PLGA),<sup>[3–5]</sup>

poly( $\epsilon$ -caprolactone),<sup>[6–8]</sup> and poly(2-hydroxyethyl methacrylate) (PHEMA)<sup>[9–12]</sup> have demonstrated some potential or promising results in the development of devices for drug delivery<sup>[13]</sup> or scaffolds for tissue engineering applications.<sup>[14]</sup> They have notably been used for the encapsulation and controlled release of several drugs/proteins, such as heparin,<sup>[15]</sup> bovine serum albumin (BSA),<sup>[16]</sup> metronidazole antibiotic,<sup>[17]</sup> and many more.<sup>[18]</sup>

Over the last decade, the preparation of doubly porous materials has particularly attracted the focus of researchers for the design of biocompatible scaffolds meant for biomedical applications.<sup>[19]</sup> A hierarchical double porosity may constitute a real benefit in the area of tissue engineering as the first porosity with pore sizes higher than 100  $\mu\text{m}$  may enable the seeding and proliferation of suitable cell lines within the material, while the second porosity with pore diameters lower than 1  $\mu\text{m}$  should permit to improve the nutrient and waste flow through the material when the macropores are clogged at the last stage of

Institut de Chimie et des Matériaux Paris-Est, CNRS – Université Paris-Est Créteil Val-de-Marne, 2, rue Henri Dunant 94320, Thiais, France  
E-mail: grande@icmpe.cnrs.fr

the cell culture. In this context, different methodologies have hitherto been developed for the design and synthesis of such materials displaying a double porosity. Temperature-induced phase separation (TIPS) in combination with particle leaching has recently been reported for the design of poly(L-lactic acid) (PLLA),<sup>[20]</sup> gelatin<sup>[21]</sup> or PLGA<sup>[22]</sup> scaffolds. In these studies, poly(ethyl methacrylate), paraffin, and sucrose spheres (with different diameter ranges) were used as the macroporogens, while dioxane, ethanol/water or chloroform allowed for the formation of small pores during the TIPS process. Gas foaming combined with particle leaching also seems to be appropriate for the preparation of doubly porous PLLA- and PLGA-based frameworks when using dioxane/water as a porogenic solvent mixture and sodium bicarbonate particles.<sup>[23]</sup> The design of doubly porous materials was also investigated by a double porogen approach. In this case, PLLA scaffolds were prepared by using a macromolecular porogen, *i.e.* poly(ethylene glycol), in combination with NaCl particles.<sup>[24]</sup> On the other hand, superporous PHEMA scaffolds were produced through the use of NaCl or  $(\text{NH}_4)_2\text{SO}_4$  macroporogens in conjunction with cyclohexanol/dodecan-1-ol as a porogenic solvent mixture.<sup>[25]</sup> In addition, High Internal Phase Emulsion (HIPE) templating has allowed for the generation of PHEMA-based materials presenting a hierarchically-structured porosity.<sup>[26–28]</sup>

In order to develop more robust and versatile approaches to biocompatible doubly porous PHEMA-based materials, we propose novel synthetic strategies through the use of two distinct types of porogens, namely a macroporogen in combination with a nanoporogen. To generate the macroporosity, either sieved  $\text{CaCO}_3$  particles in the 125–160  $\mu\text{m}$  range or 200–250  $\mu\text{m}$  sieved PMMA beads are used, while the second porosity is obtained by using either hydroxyapatite (HA) nanoparticles (200 nm) or a porogenic solvent, such as ethanol. Such straightforward methodologies based upon porogen remov-

al allow for the preparation of relatively well-defined doubly porous PHEMA-based materials. The porosity of the as-obtained porous frameworks is characterized by means of mercury intrusion porosimetry (MIP) and scanning electron microscopy (SEM). Finally, the possibility to further functionalize such materials is investigated through an activation of hydroxyl groups, and subsequent coupling with a model amine, *i.e.* propargylamine. The achievement of the functionalization is confirmed by Raman spectroscopy.

## Experimental Part

### Materials

2-hydroxyethyl methacrylate (HEMA, 97%), ethylene glycol dimethacrylate (EGDMA, 98%), hydroxyapatite (HA, average particle size equal to 200 nm) and 1,1'-carbonyl diimidazole (CDI,  $\geq 97\%$ ) were purchased from Aldrich. 2,2'-Azobis(2-methylpropionitrile) (AIBN, 98%, Aldrich) was recrystallized from methanol (MeOH) prior to use. 2-Acrylamido-2-methylpropane sulfonic acid tetrabutylammonium salt (AMPS-TBA) was prepared by a classical ion-exchange reaction from 2-acrylamido-2-methylpropane sulfonic acid (AMPS, 98%, Fluka). Calcium carbonate ( $\text{CaCO}_3$ , Mikhart 130, particle size ranging from 60 to 400  $\mu\text{m}$ ) was kindly provided by Provençale SA, France, and sieved (125–160  $\mu\text{m}$ ), prior to PHEMA-based material synthesis. Poly(methyl methacrylate) (PMMA) beads (200  $\mu\text{m}$  average diameter,  $D = 3.0$ ) were obtained from Polysciences, Inc., and sieved (200–250  $\mu\text{m}$ ), prior to PHEMA-based material synthesis. Absolute ethanol (EtOH, 99%, SDS), MeOH (99%, SDS), dichloromethane ( $\text{CH}_2\text{Cl}_2$ , 99.9%, Carlo Erba), tetrahydrofuran (THF, 99.9%, SDS) were used without any further purification procedure. Hydrochloric acid (HCl, 37 wt %, Normapur) was diluted to prepare a 3 M aqueous solution.

### Preparation of Biporous PHEMA-Based

#### Material using $\text{CaCO}_3$ and HA as Porogens

$\text{CaCO}_3$  particles and HA nanoparticles were mixed in glass vials with a polymerization

mixture constituted of HEMA (0.9 g, 6.92 mmol), EGDMA (0.152 g, 0.77 mmol, HEMA/EGDMA molar ratio: 90/10), AMPS-TBA (35 mg, 1 mol % with respect to comonomers), and AIBN (42 mg, 2 wt % with respect to comonomers). The final comonomers/ $\text{CaCO}_3$ /HA mass ratio was equal to 4/1/1. The vials were first placed in a UV oven for 1 h at 365 nm for pre-polymerization, and then they were transferred to an oil bath at 70 °C for 4 h in order to complete the polymerization. After polymerization, the materials were subjected to an acidic hydrolysis by immersing them in a 3 M HCl solution at room temperature for a 1 week period. The hydrolysis solution was changed every 2 days. After hydrolysis, the samples were abundantly washed with deionized water, and dried at room temperature under vacuum.

#### **Preparation of Biporous PHEMA-Based Material Using $\text{CaCO}_3$ and Ethanol as Porogens**

A mixture of HEMA (0.9 g, 6.92 mmol), EGDMA (0.152 g, 0.77 mmol, HEMA/EGDMA molar ratio: 90/10), and AMPS-TBA (35 mg, 1 mol % with respect to comonomers) were homogeneously mixed at room temperature with AIBN (2 wt % with respect to comonomers) and absolute ethanol (0.343 mL) as a porogenic solvent. The mixture was then poured into a cylinder-shaped vial with calcium carbonate particles, put into a UV oven for 1 h irradiating at 365 nm, and finally heated to 70 °C for 4 h. The final comonomers/ $\text{CaCO}_3$ /ethanol mass ratio was equal to 4/1/1. After polymerization, a 3 M HCl solution was used to hydrolyze calcium carbonate particles, the hydrolysis solution being renewed every 2 days for 1 week. The samples were washed abundantly with deionized water, filtered off, and finally dried under vacuum at room temperature overnight.

#### **Preparation of Biporous PHEMA-Based Material using PMMA Beads as Macroporogens**

First of all, PMMA beads were introduced into vials and sintered in a vacuum oven at

140 °C for 19 h. The polymerization mixture that consisted of HEMA (0.9 g, 6.92 mmol), EGDMA (0.152 g, 0.77 mmol, HEMA/EGDMA molar ratio: 90/10), AMPS-TBA (35 mg, 1 mol % with respect to comonomers), and AIBN (42 mg, 2 wt %) was added to the as-obtained PMMA continuous phase, and the polymerization was conducted at 70 °C for 4 h. The final comonomers/PMMA beads mass ratio was equal to 1/2. The PMMA beads were removed by extraction with a suitable solvent (THF or  $\text{CH}_2\text{Cl}_2$ ) at room temperature for approximately 3 days. The extracting solvent was changed twice a day in order for the porogen extraction to proceed faster. After this step, the samples were washed abundantly with the extracting solvent, and dried at room temperature under vacuum.

#### **Functionalization of Doubly Porous PHEMA-Based Material**

114 mg of porous PHEMA-based material (~1 mmol of hydroxyl groups) was suspended in 3 mL of acetone. 324 mg of CDI (2 equiv. with respect to the total hydroxyl groups) was added, and the reaction was gently stirred on an orbital shaking plate overnight. The solid was filtered off and abundantly washed with acetone. After resuspension in 3 mL of acetone, propargylamine (275 mg, 5 equiv. with respect to the initial hydroxyl groups) was added, and the solution was gently shaken for 24 h at room temperature. After abundant washing with acetone and methanol, the resulting alkyne-functionalized biporous PHEMA material was recovered, and analyzed by Raman spectroscopy.

#### **Instrumentation**

Sintering of PMMA beads was realized in a Solvis LAB VC-20 vacuum oven from Penggli coupled with a CIT Alcatel pump type 2002A. The photoinitiated free-radical copolymerization was performed in a Spectrolinker XL-1500 UV oven from Spectronics equipped with six 15 W lamps irradiating at 365 nm.  $^1\text{H}$  NMR analyses were realized on a Bruker Avance II

spectrometer operating at a resonance frequency of 400 MHz at room temperature using MeOD as the deuterated solvent. Infrared spectra were recorded using a Bruker Tensor 27 DTGS spectrometer in attenuated total reflection (ATR) mode between 4000 and 450  $\text{cm}^{-1}$  with an average of 32 consecutive scans and a resolution of 4  $\text{cm}^{-1}$ . Raman characterization of the functional materials was carried out using a LabRAM HR spectrometer from Horiba JobinYvon equipped with a laser emitting at 633 nm. SEM investigations of the materials were performed with a LEO 1530 microscope equipped with InLens and SE2 detectors using a low accelerating tension (2 kV) with a diaphragm aperture of 30  $\mu\text{m}$ . Prior to analyses, the samples were cryo-fractured and coated with a 4-nm layer of palladium/platinum alloy in a Cressington 208 HR sputter-coater. The porosity ratio, pore volume, and pore size distribution of the materials were determined by MIP using an AutoPore IV 9500 porosimeter from Micromeritics. The determination of this porosity features was based on the Washburn equation between the applied pressure (from 1.03 to 206.8 MPa) and the pore diameter into which mercury intrudes.

## Results and Discussion

In order to develop biocompatible doubly porous materials, 2-hydroxyethyl methacrylate (HEMA) was chosen as the monomer of reference, as it has been so far mainly devoted to the preparation of scaffolds for tissue engineering or the production of drug delivery devices. PHEMA-based materials have notably been used as hydrogels to develop soft contact and intraocular lenses, implants, wound dressings, drug delivery systems, and carriers for immobilization of enzymes, antibodies, or cells.<sup>[29]</sup> On the other hand, hydroxyl groups in such materials are available for further modifications to promote cell attachment, proliferation, differentiation, and migration in biomedical

applications.<sup>[30–32]</sup> Ethylene glycol dimethacrylate (EGDMA) was chosen as the cross-linking agent as its use in combination with HEMA has been well reported. In addition, tiny quantities (1 mol % with respect to monomer and cross-linker) of a charged co-monomer, *i.e.* 2-acrylamido-2-methylpropane sulfonic acid tetrabutylammonium salt (AMPS-TBA), were used as it would allow for the decoration of the pore surface with charges for potential further functionalization or even for the generation of an electro-osmotic flow (EOF) through the polymeric frameworks, which could be of interest for the design of specific bioreactors.<sup>[33,34]</sup>

### Use of $\text{CaCO}_3$ for Macropore Generation

In a first attempt to design materials with double porosity,  $\text{CaCO}_3$  particles with size ranging from 125 to 160  $\mu\text{m}$  were used to generate the macroporosity as they have recently been demonstrated to allow for the formation of porous hydrogels through particle templating.<sup>[35]</sup> In addition, HA nanoparticles, with an average diameter of 200 nm, were selected as nanoporogenic agents for the first time, because they can easily be removed under the same hydrolytic conditions as those used for  $\text{CaCO}_3$  removal. A mixture of HEMA, EGDMA, and AMPS-TBA was copolymerized *via* AIBN-induced free-radical polymerization in presence of the pair of porogens, *i.e.*  $\text{CaCO}_3$  and HA. After polymerization at 70 °C for 4 h, the resulting materials were subjected to a hydrolysis in a 3 M HCl aqueous solution for 1 week. The complete removal of the porogenic templates was verified by FTIR spectroscopy through the total disappearance of the characteristic bands of HA at  $\sim 1020 \text{ cm}^{-1}$  and  $\text{CaCO}_3$  at  $\sim 1400 \text{ cm}^{-1}$ , respectively (Figure 1).

In addition, FTIR confirmed that the hydrolysis, carried out in rather harsh acidic conditions, did not affect the material structure. Indeed, the C=O stretching band intensity at 1720  $\text{cm}^{-1}$  from the PHEMA network did not show any significant decrease after porogen removal. The porosity was characterized by MIP and SEM

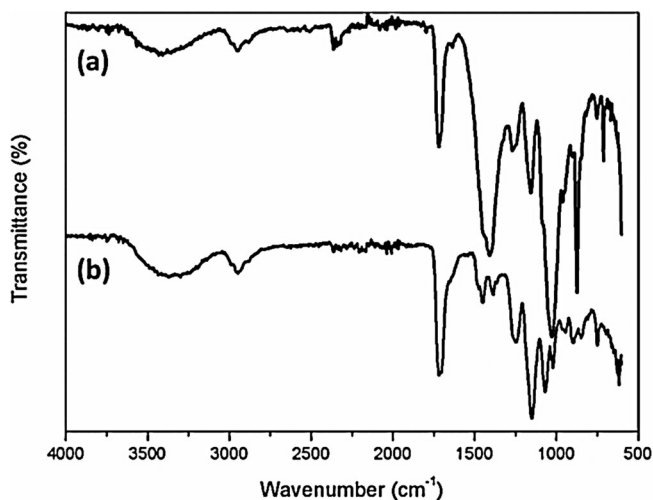


**Figure 1.**

ATR-FTIR spectra of PHEMA-based material before (a) and after (b) hydrolysis of the porogenic agents ( $\text{CaCO}_3$  and HA).

(Figure 2). MIP evidenced the presence of a bimodal porosity, the macroporosity being centered around  $100\ \mu\text{m}$ , while the smaller porosity was found to be centered around  $1.5\ \mu\text{m}$ . It was thus assumed that the

porosity centered on  $1.5\ \mu\text{m}$ , arising from the hydrolysis of the  $200\ \text{nm}$  HA particles, was due to HA cluster formation during the polymerization process, giving rise to a higher average pore size than that expected.

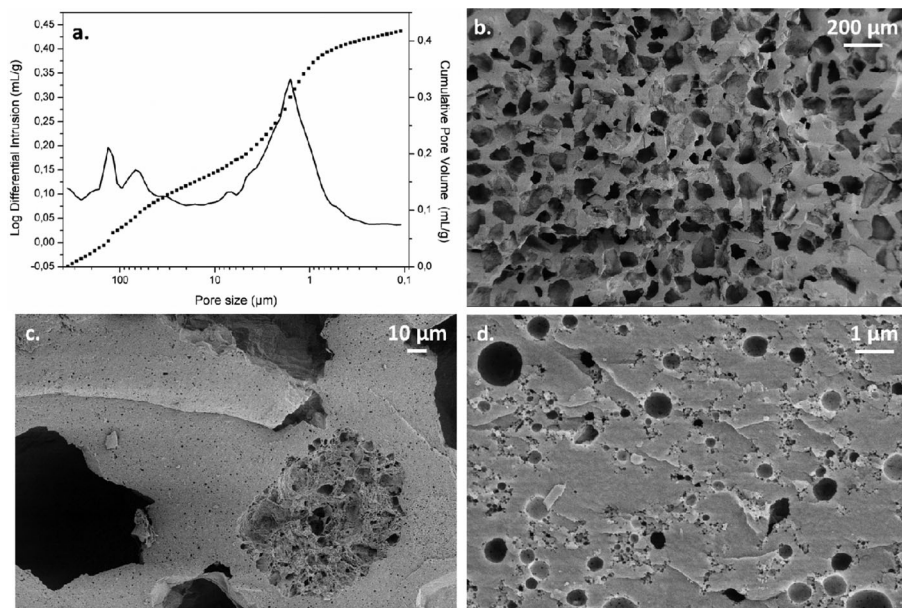


**Figure 2.**

MIP profile (a) and SEM images (b,c,d) of doubly porous PHEMA-based material obtained upon hydrolysis of  $\text{CaCO}_3$  and HA by aqueous HCl solution.

Moreover, MIP analysis may suggest a collapse of the macroporosity during the measurements, as evidenced in the porosity profile of the PHEMA-based material by a couple of peaks between 30 and 200  $\mu\text{m}$ .

SEM observation of this porous material corroborated MIP analysis. Indeed, macropores with an average diameter around 120  $\mu\text{m}$  were observed along with a smaller porosity centered around 1.05  $\mu\text{m}$ .

In order to circumvent the HA cluster formation, and thus to obtain smaller pores, another porogen system, still based on the use of  $\text{CaCO}_3$  particles as a macroporogenic agent, was investigated. In this case, a porogenic solvent, *i.e.* ethanol, was used instead of HA nanoparticles. As previously described, monomers, cross-linker, porogenic agents, and free-radical initiator were mixed together in glass vials, and the polymerization was triggered by UV irradiation for 1 h at 365 nm, and then heating at 70  $^\circ\text{C}$  for 4 h. The acidic treatment of the materials enabled the generation of porous PHEMA frameworks. Again, FTIR confirmed the complete hydrolysis of  $\text{CaCO}_3$

particles and the total removal of ethanol, while the integrity of the chemical structure of the materials was not altered in such harsh conditions (data not shown). A nicely well-defined bimodal porous distribution was evidenced by MIP analysis (Figure 3), thus demonstrating the possibility to easily generate such biporous materials. The obtained material displayed a porosity ratio of 61% with an equal amount of macropores and nanopores, which was consistent with the 1/1 macroporogen/nanoporogen ratio in the precursory network.

SEM observation of the as-obtained PHEMA-based scaffolds demonstrated the generation of a bimodal porous profile with a macroporosity centered around 170  $\mu\text{m}$  and a nanoporosity on 440 nm (Figure 3). Further, complementary measurements performed by helium pycnometry strongly suggested that the newly generated biporous materials were characterized by open pore structures with interconnected channels through which a fluid (helium) could flow. Indeed, the true density value at 25  $^\circ\text{C}$  associated with a typical biporous network

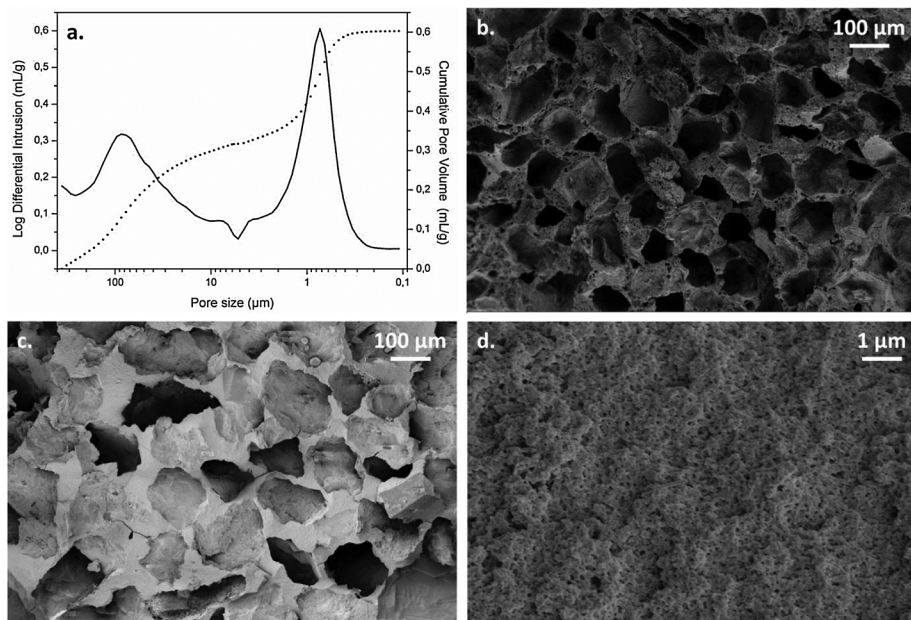


**Figure 3.**

MIP profile (a) and SEM images (b,c,d) of doubly porous PHEMA-based material obtained upon removal of  $\text{CaCO}_3$  and ethanol.

( $1.165 \text{ g.cm}^{-3}$ ) was very close to that of the corresponding non-porous network as a reference system ( $1.170 \text{ g.cm}^{-3}$ ).

### Use of PMMA Beads for Macropore Generation

The second strategy developed to generate doubly porous polymeric scaffolds was adapted from a previously published work from LaNasa et al.,<sup>[36]</sup> in which PMMA beads were used to generate an interconnected macroporous network within PHEMA hydrogels, after extraction. The main difference from this previous work relied on the generation of nanoporosity within the same material.

Prior to the formation of the PHEMA network, PMMA beads, displaying an average diameter of  $200 \mu\text{m}$ , were first sieved because of their broad particle size distribution ( $\mathcal{D} = 3.0$ ). Depending on the bead average diameter, different fractions were isolated, and the fraction comprising beads with diameters ranging from  $200$  to  $250 \mu\text{m}$  was used for further experiments. PMMA beads ( $\varnothing = 200\text{--}250 \mu\text{m}$ ) were then sintered for 19 h at  $140^\circ\text{C}$ , *i.e.* a temperature higher than their glass transition temperature ( $T_g = 105^\circ\text{C}$ ). The formation of the PMMA beads template was monitored by SEM (Figure 4).

As expected, a coalescence of PMMA spheres was observed, giving rise to a continuous phase that should further lead to interconnected pores after cross-linked PHEMA synthesis, followed by PMMA beads extraction. The vial containing the

PMMA beads template was filled with the polymerization feed. The free-radical copolymerization of HEMA, EGDMA, and AMPS-TBA was carried out at  $70^\circ\text{C}$  for 4 h. After subsequent extraction of PMMA beads which were soluble in a suitable solvent, the complete extraction of the macroporogenic agent was confirmed by gravimetry. The resulting porous materials were characterized by MIP and SEM (Figure 5). It was immediately noticed that the use of highly polar solvents was detrimental to the robustness of PHEMA-based materials, likely due to an important swelling that physically destroyed the structure of the as-obtained materials. However, the use of dichloromethane or THF as extracting solvents for PMMA beads allowed for the preparation of much more stable materials. Surprisingly, both SEM observation and MIP analysis of the materials revealed the presence of two porosity levels, even though no specific nanoporogen was used in the precursory networks. MIP analysis of these materials showed a well-defined interconnected macroporosity centered around  $90 \mu\text{m}$ , while a second level of porosity was found around  $20 \text{ nm}$ , and was probably generated during the macroporogen extraction step due to the possible microporogen role played by the extracting solvent. It is noteworthy that the corresponding PHEMA-based material before extraction of PMMA beads did not show one such level of nanoporosity.

These original biporous PHEMA-based materials presented a 60% porosity, and an equal amount of macropores and nanopores.

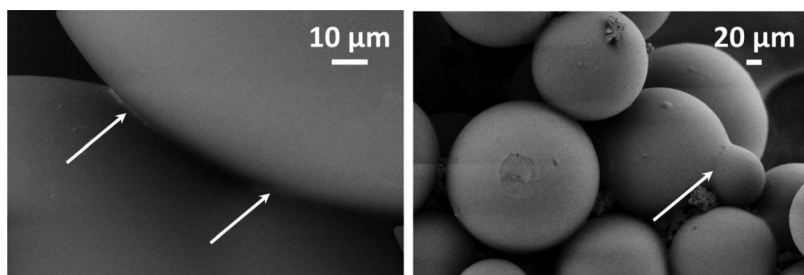


**Figure 4.**

SEM micrographs of PMMA beads obtained after sintering (white arrows highlight the coalescence of PMMA beads).

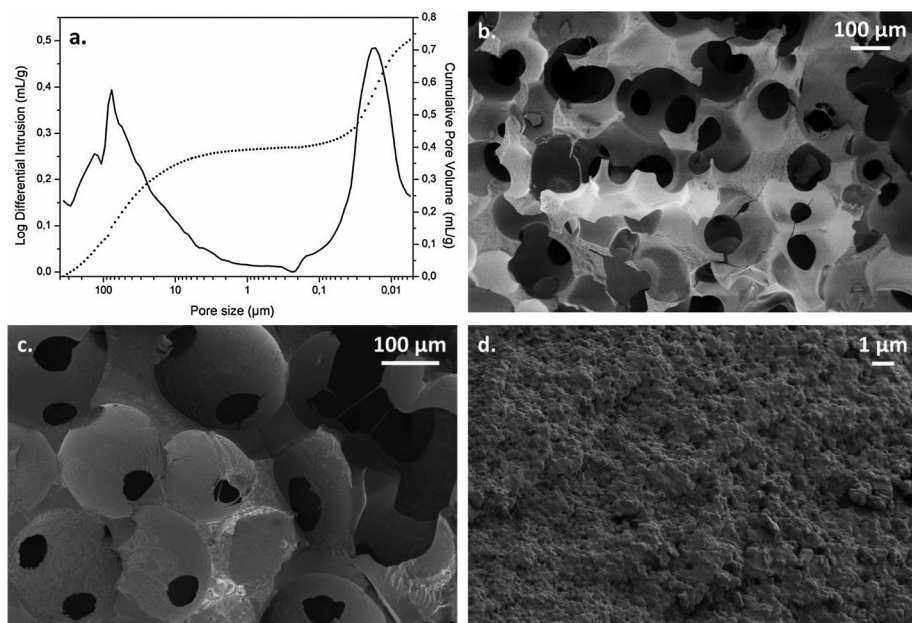


**Figure 5.**

MIP profile (a) and SEM micrographs (b) of porous PHEMA-based material obtained upon extraction of PMMA beads with THF.

The SEM observation confirmed the presence of a bimodal porosity (Figure 5). Macropores with an average diameter of about 195 μm and interconnecting voids of about 65 μm were observed, while nanopores in the 360 nm range were found. It should be stressed that the significant difference between the results obtained from the two characterization techniques might be attributable to the pressure applied on these soft materials (due to Hg penetration under high pressure) that could lead to partial collapse of the porosity, and thus to underestimation and inaccuracy in the determination of pore size distributions.<sup>[37]</sup> In addition, the true density value at 25 °C associated with a typical biporous material (1.161 g.cm<sup>-3</sup>) was comparable with that of the corresponding non-porous network (1.170 g.cm<sup>-3</sup>), thus confirming the interconnection of the pores.

#### Functionalization of Doubly Porous PHEMA-Based Material

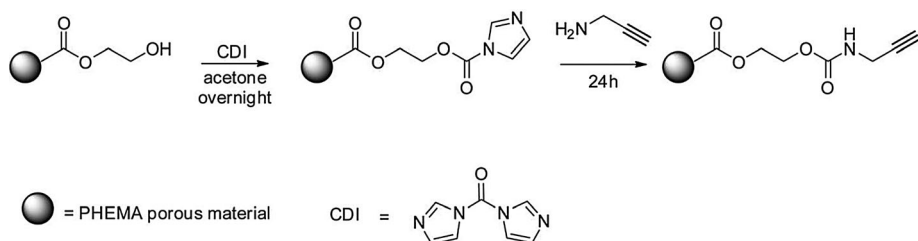
The availability of the hydroxyl functions at the pore surface, and thus the possibility to

tether interesting biological molecules, such as growth factors or peptides, onto the pores was assessed by a two-step chemical modification involving activation of hydroxyl groups with carbonyl diimidazole (CDI), followed by subsequent coupling with a model compound, *i.e.* propargylamine (Figure 6).

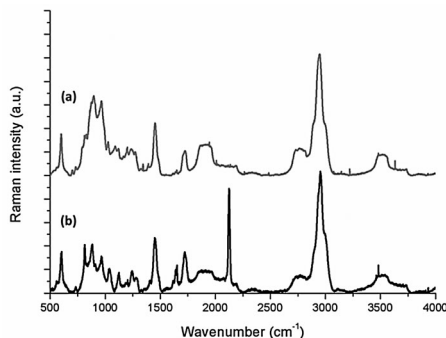
A biporous PHEMA-based material was gently stirred in acetone at room temperature before the addition of CDI. Upon stirring overnight at room temperature, the material was washed abundantly with acetone and resuspended in the same solvent. The successive addition of propargylamine and stirring for 24 h afforded the alkyne-modified material. A blank experiment, in which no CDI activation was carried out before the coupling step, was also realized.

Raman spectroscopy confirmed that the covalent attachment of propargylamine was only achieved during the two-step reaction. Indeed, Raman spectra showed a characteristic intense band at 2100 cm<sup>-1</sup> corresponding to the terminal alkyne stretching



**Figure 6.**

Synthetic pathway adopted for the functionalization of porous PHEMA networks.

**Figure 7.**

Raman spectra of PHEMA network in the presence of propargylamine without CDI activation –blank experiment– (a) and alkyne-modified PHEMA (b).

band ( $\nu_{\text{C}\equiv\text{C}-\text{H}}$ ) (Figure 7b), whereas it was not present either in the product resulting from the blank experiment (Figure 7a) or in the starting PHEMA-based material (data not shown).

## Conclusion

This paper illustrates the effectiveness and versatility of original porogen templating approaches as straightforward routes to doubly porous PHEMA-based materials. Such biporous materials could successfully be engineered through the use of either  $\text{CaCO}_3$  particles or PMMA beads as macroporogens, in conjunction with HA nanoparticles or a solvent as nanoporogens. Upon removal of the porogenic agents, such doubly porous polymeric frameworks were indeed obtained, and the dual porosity was confirmed by MIP and SEM character-

ization. Further, the possibility to functionalize them with a model compound was attested *via* a straightforward two-step chemical modification that allows for further thiol-yne “click” chemistry conjugation with molecules of biological interest, for instance.

The two levels of porosity could make these materials suitable for miscellaneous applications in the biomedical area. These porous materials could thus constitute attractive scaffolds for tissue engineering applications as long as bioactive molecules, such as growth factors, are grafted at the pore surface. Finally, the possibility to generate an electro-osmotic flow through the (nano)porosity will be investigated in order to demonstrate that the charges brought by the AMPS-TBA co-monomer are incorporated at the pore surface, and that the resulting materials may be used as potential bioreactors.

**Acknowledgements:** The authors thank the CNRS and the University Paris-Est Créteil for financial support. They are grateful to R. Pirès and M. Guerrouache (CNRS, Thiais) for their kind assistance with SEM experiments and Raman spectroscopy, respectively.

- [1] C. J. Brinker, *Curr. Opin. Solid State Mater. Sci.* **1996**, 1, 798.
- [2] D. Wu, F. Xu, B. Sun, R. Fu, H. He, K. Matyjaszewski, *Chem. Rev.* **2012**, 112, 3959.
- [3] C. R. Chu, R. D. Coutts, M. Yoshioka, F. L. Harwood, A. Z. Monosov, D. Amiel, *J. Biomed. Mater. Res.* **1995**, 29, 1147.
- [4] L. Lu, S. J. Peter, M. D. Lyman, H.-L. Lai, S. M. Leite, J. A. Tamada, S. Uyama, J. P. Vacanti, L. Robert, A. G. Mikos, *Biomaterials* **2000**, 21, 1837.
- [5] J. K. Sherwood, S. L. Riley, R. Palazzolo, S. C. Brown, D. C. Monkhouse, M. Coates, L. G. Griffith, L. K. Landeen, A. Ratcliffe, *Biomaterials* **2002**, 23, 4739.
- [6] G. Ciapetti, L. Ambrosio, L. Savarino, D. Granchi, E. Cenni, N. Baldini, S. Pagani, S. Guizzardi, F. Causa, A. Giunti, *Biomaterials* **2003**, 24, 3815.
- [7] I. Zein, D. W. Hutmacher, K. C. Tan, S. H. Teoh, *Biomaterials* **2002**, 23, 1169.
- [8] M. Shin, H. Yoshimoto, J. P. Vacanti, *Tissue Eng.* **2004**, 10, 33.
- [9] J. Hradil, D. Horák, *React. Funct. Polym.* **2005**, 62, 1.
- [10] J. S. Belkas, C. A. Munro, M. S. Shoichet, M. Johnston, R. Midha, *Biomaterials* **2005**, 26, 1741.
- [11] S. A. Bencherif, N. R. Washburn, K. Matyjaszewski, *Biomacromolecules* **2009**, 10, 2499.
- [12] Š. Kubinová, D. Horák, E. Syková, *Biomaterials* **2009**, 30, 4601.
- [13] L. S. Nair, C. T. Laurencin, *Prog. Polym. Sci.* **2007**, 32, 762.
- [14] R. Langer, J. P. Vacanti, *Science* **1993**, 260, 920.
- [15] M. R. Kreitz, J. A. Domm, E. Mathiowitz, *Biomaterials* **1997**, 18, 1645.
- [16] Y.-Y. Yang, T.-S. Chung, N. Ping Ng, *Biomaterials* **2001**, 22, 231.
- [17] V. R. Patel, M. M. Amiji, *Pharm. Res.* **1996**, 13, 588.
- [18] S.-H. Lee, H. Shin, *Adv. Drug Delivery Rev.* **2007**, 59, 339.
- [19] X. Liu, P. Ma, *Ann. Biomed. Eng.* **2004**, 32, 477.
- [20] V. A. Santamaría, H. Deplaine, D. Mariggió, A. R. Villanueva-Molines, J. M. García-Aznar, J. L. Gomez-Ribelles, M. Doblaré, G. G. Ferrer, I. Ochoa, *J. Non-Cryst. Solids* **2012**, 358, 3141.
- [21] X. Liu, P. X. Ma, *Biomaterials* **2009**, 30, 4094.
- [22] Y. Yang, J. Zhao, Y. Zhao, L. Wen, X. Yuan, Y. Fan, *J. Appl. Polym. Sci.* **2008**, 109, 1232.
- [23] K. Park, H. J. Jung, J. S. Son, K. D. Park, J.-J. Kim, K.-D. Ahn, D. K. Han, *Macromol. Symp.* **2007**, 249–250, 145.
- [24] S. Ghosh, J. C. Viana, R. L. Reis, J. F. Mano, *J. Mater. Sci.: Mater. Med.* **2007**, 18, 185.
- [25] D. Horák, H. Hlídková, J. Hradil, M. Lapčíková, M. Šlouf, *Polymer* **2008**, 49, 2046.
- [26] M. Paljevac, K. Jeřábek, P. Krajnc, *J. Polym. Environ.* **2012**, 20, 1095.
- [27] O. Kulygin, M. S. Silverstein, *Soft Matter* **2007**, 3, 1525.
- [28] N. R. Cameron, *Polymer* **2005**, 46, 1439.
- [29] N. A. Peppas, “*Hydrogels in Medicine and Pharmacy*”, CRC Press, Boca Raton, FL **1986**.
- [30] J. Yang, P. Zhang, L. Tang, P. Sun, W. Liu, P. Sun, A. Zuo, D. Liang, *Biomaterials* **2010**, 31, 144.
- [31] K. Yamada, Y. Iizawa, J.-i. Yamada, M. Hirata, *J. Appl. Polym. Sci.* **2006**, 102, 4886.
- [32] S. L. McArthur, M. W. Halter, V. Vogel, D. G. Castner, *Langmuir* **2003**, 19, 8316.
- [33] T. Lemaire, J. Kaiser, S. Naili, V. Sansalone, *Mech. Res. Commun.* **2010**, 37, 495.
- [34] T. Lemaire, S. Naili, V. Sansalone, *An. Acad. Bras. Cienc.* **2010**, 82, 127.
- [35] M. Behra, S. Schmidt, J. Hartmann, D. V. Volodkin, L. Hartmann, *Macromol. Rapid Commun.* **2012**, 33, 1049.
- [36] S. M. LaNasa, I. T. Hoffercker, S. J. Bryant, *J. Biomed. Mater. Res. Part B Appl. Biomater.* **2011**, 96B, 294.
- [37] S. Blacher, V. Maquet, R. Pirard, J. P. Pirard, R. Jérôme, *Coll. Surf. A: Physicochem. Eng. Aspects* **2001**, 187–188, 375.